

Multi-Class Segmentation from Aerial Views using Recursive Noise Diffusion

Benedikt Kolbeinsson
 Imperial College London
 bk915@imperial.ac.uk

Krystian Mikolajczyk
 Imperial College London
 k.mikolajczyk@imperial.ac.uk

Abstract

Semantic segmentation from aerial views is a vital task for autonomous drones as they require precise and accurate segmentation to traverse safely and efficiently. Segmenting images from aerial views is especially challenging as they include diverse view-points, extreme scale variation and high scene complexity. To address this problem, we propose an end-to-end multi-class semantic segmentation diffusion model. We introduce recursive denoising which allows predicted error to propagate through the denoising process. In addition, we combine this with a hierarchical multi-scale approach, complementary to the diffusion process. Our method achieves state-of-the-art results on UAVid and on the Vaihingen building segmentation benchmark. Code and models are available here: <https://github.com/benedikt-kol/recursive-noise-diffusion>

1. Introduction

Fully autonomous drones, also known as unmanned aerial vehicles (UAVs), have many socially and economically important applications, such as: infrastructure inspection, agriculture monitoring, search and rescue, disaster management, surveying and delivery services. However, for drones to perform these tasks autonomously they need to understand their environment [15]. Semantic segmentation is the task of labeling each pixel within an image to a class (e.g., “person” or “tree”) and is crucial for drones. Segmenting images from aerial views is especially challenging as they include diverse view-points, extreme scale variation and high scene complexity [23].

Conventional methods typically utilize convolutional neural network (CNN) with an encoder-decoder structure, such as U-Net [30]. A limited receptive field will struggle with large scale variations, for example detecting large objects benefits from more global features while smaller objects are often better predicted using larger image sizes [36]. To overcome these limitations it is common to use multi-scale features [14, 25]. Combining scales by averaging the output from different scales at inference works but is im-

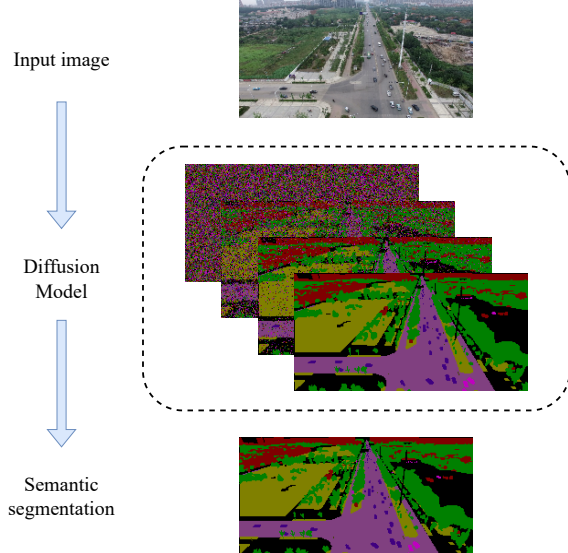


Figure 1. Generating a semantic segmentation map using a diffusion model conditioned on an image.

proved when the scale combination is learned [7, 36].

To address this problem, we propose a hierarchical multi-scale diffusion model, which naturally learns how to combine multi-scale predictions (shown in Figure 1). This is made possible as we introduce a novel training method called *recursive denoising*, which allows a diffusion model to learn to use additional information during inference. We discuss the details of our method in Section 3 and we show our method achieves state-of-the-art results on both UAVid [23] and Vaihingen Buildings [11] in Section 4.

Our main contributions are:

- We propose a multi-class segmentation model using Recursive Noise Diffusion.
- We introduce *recursive denoising*, which allows information to propagate through the denoising process, along with a hierarchical multi-scale approach.
- We achieve state-of-the-art results on UAVid and Vaihingen Buildings.

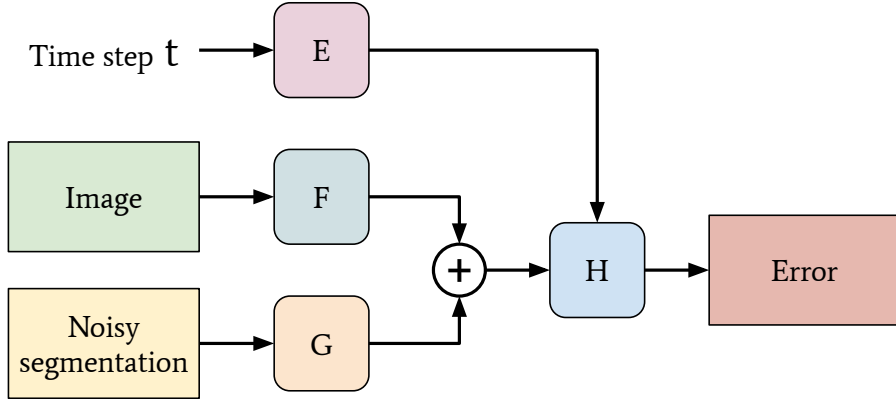


Figure 2. Diagram of our diffusion model. The inputs are an RGB image, one-hot encoded noisy segmentation and a time step t . The output is the predicted noise on the noisy segmentation. The method is discussed in Section 3 and architecture details can be found in Section 3.4.

2. Related Work

Semantic Segmentation Long *et al.* [20] introduced fully convolutional networks for semantic segmentation, which became a fundamental building block for future methods [5, 6, 27]. Pyramid pooling has been used to increase the receptive field of a network and is used in PSPNet [43] and DeepLab [8]. Tao *et al.* [36] and Chen *et al.* [7] use multi-scale attention to increase the network’s receptive field. Transformers [38] are extensively used for segmentation [35, 39, 40, 44].

Diffusion Denoising diffusion probabilistic models (DDPM), also known simply as diffusion models, are a type of generative models. Initially proposed by Sohl-Dickstein *et al.* [33], they have become state-of-the-art as they have been shown to outperform GANs [13]. Thus, they have recently become exceedingly popular for image generation [12, 28, 29, 31]. We discuss the theory behind diffusion models in Section 2.1.

Segmentation using generative methods Generative adversarial networks (GANs) [16] have been used for semantic segmentation [22, 34, 42]. GANs have also been used to generate synthetic data to train segmentation models [4, 37]. Baranchuk *et al.* [3] have used intermediate representations from a pre-trained diffusion model to perform semantic segmentation. Amit *et al.* [1] train a diffusion model to perform segmentation but only for binary classification. We propose modifications to diffusion models which allow us to perform full multi-class semantic segmentation. We show our method outperforms their method on Vaihingen building dataset in Section 4.

2.1. Diffusion Theory

Diffusion models consist of two processes, first the *diffusion process* or *forward process* q , a Markov chain which gradually adds Gaussian noise to the data. Given a data distribution $\mathbf{x}_0 \sim q(\mathbf{x}_0)$, we define q as:

$$q(\mathbf{x}_{1:T}|\mathbf{x}_0) = \prod_{t=1}^T q(\mathbf{x}_t|\mathbf{x}_{t-1}) \quad (1)$$

$$q(\mathbf{x}_t|\mathbf{x}_{t-1}) = \mathcal{N}(\mathbf{x}_t; \sqrt{1 - \beta_t} \mathbf{x}_{t-1}, \beta_t \mathbf{I}) \quad (2)$$

Where $\beta_t \in (0, 1)$ is the noise schedule, $\mathbf{x}_1, \dots, \mathbf{x}_T$ are latent variables and T is the number of time steps. The latent \mathbf{x}_T is approximately an isotropic Gaussian distribution, given a sufficiently large T .

The second process, called the *denoising process* or *reverse process* p , is also defined as a Markov chain starting at $p_\theta(\mathbf{x}_T) = \mathcal{N}(\mathbf{x}_T; \mathbf{0}, \mathbf{I})$ but learns to gradually remove Gaussian noise:

$$p_\theta(\mathbf{x}_{0:T}) = p_\theta(\mathbf{x}_T) \prod_{t=1}^T p_\theta(\mathbf{x}_{t-1}|\mathbf{x}_t) \quad (3)$$

$$p_\theta(\mathbf{x}_{t-1}|\mathbf{x}_t) = \mathcal{N}(\mathbf{x}_{t-1}; \mu_\theta(\mathbf{x}_t, t), \Sigma_\theta(\mathbf{x}_t, t)) \quad (4)$$

Interestingly, given $\alpha_t = 1 - \beta_t$ and $\bar{\alpha}_t = \prod_{s=0}^t \alpha_s$, sampling \mathbf{x}_t at arbitrary timestep t is achieved with:

$$q(\mathbf{x}_t|\mathbf{x}_0) = \mathcal{N}(\mathbf{x}_t; \sqrt{\bar{\alpha}_t} \mathbf{x}_0, (1 - \bar{\alpha}_t) \mathbf{I}) \quad (5)$$

Further details on the theory behind diffusion models may be found in [19, 26]. However, Bansal *et al.* [2] calls this theory into question. They show diffusion models can be trained without Gaussian noise and even with deterministic image degradation. We are inspired by their work, and

thus we propose to use a diffusion model to predict semantic segmentation maps. Converting diffusion models from typical generative tasks, to a predictive task, involves modifying the *diffusion process* and the *denoising process*. We discuss the details in Section 3.

3. Recursive denoising

Given an aerial RGB image $\mathbf{x} \in \mathbb{R}^{W \times H \times 3}$, our goal is to predict a semantic segmentation map $\mathbf{s} \in \mathbb{R}^{W \times H \times d_{\text{classes}}}$, with corresponding class labels for each pixel. Where W, H are the width and height of the image, and d_{classes} is the total number of classes.

3.1. Multi-class diffusion

We modify the diffusion process to better suit the problem of predicting semantic segmentation. Given an image $\mathbf{x} \in \mathbf{X}$, the corresponding one-hot encoded segmentation map $\mathbf{s}_0 \in (\mathbf{S}|\mathbf{x})$ and time step (noise level) $t \in [0, T]$, we define the forward noising process q , which adds Gaussian noise with variance $\beta_t \in (0, 1)$, as follows:

$$q(\mathbf{s}_t | \mathbf{s}_{t-1}) = \mathbf{s}_{t-1} + \mathcal{N}(0, \beta_t \mathbf{I}) \quad (6)$$

We define the noise schedule β_t , as:

$$\beta_t = \frac{t}{T} \quad (7)$$

Trivially, the total added noise can be written as:

$$\epsilon_t = \mathbf{s}_t - \mathbf{s}_0 \quad (8)$$

We approximate the reverse process (denoising) using a neural network, ϵ_θ . Following Ho *et al.* [19], ϵ_θ predicts ϵ_t , meaning:

$$\epsilon_t \approx \epsilon_\theta(\mathbf{s}_t, \mathbf{x}, t) \quad (9)$$

Thus, we can predict the segmentation map at any arbitrary time step t , as follows:

$$\mathbf{s}_0 \approx \mathbf{s}_t - \epsilon_\theta(\mathbf{s}_t, \mathbf{x}, t) \quad (10)$$

For training, we use the mean squared error (MSE) of the predicted noise as our loss function:

$$L_{\text{mse}} = E_{\mathbf{s}_0, \mathbf{x}, t, \epsilon_t} [\|\epsilon_t - \epsilon_\theta(\mathbf{s}_t, \mathbf{x}, t)\|^2] \quad (11)$$

3.2. Recursive denoising

When we train the model on an arbitrary step of the noising process, as is most common [19, 26], we notice the model quickly overfits on the training data and does not generalize. We believe the binary labels allow for a trivial denoising strategy to be learned, e.g. rounding logits. This causes two issues, first, the model does not fully utilize the

conditional image but rather simply uses the noisy segmentation. Second, during testing, the model is too dependent on the initial steps in the denoising process. To solve this, we propose to train with *recursive denoising*.

Training with *recursive denoising* involves progressing through each time step t from T to 1, which allows a portion of the predicted error to propagate. It can also be used to propagate additional information which we discuss in Section 3.3. Algorithm 1 shows the process for a single training sample. This *recursive denoising* method can be thought as mimicking the testing process, as testing requires progressing through each time step.

Algorithm 1: Training with recursive denoising

Input: $\mathbf{x} \in \mathbb{R}^{W \times H \times 3}$, RGB image
Input: $\bar{\mathbf{s}} \in \mathbb{R}^{W \times H \times \text{classes}}$, segmentation labels
Parameters: $T \in \mathbb{Z}^1$, number of time steps

```

1  $\hat{\mathbf{s}}_T \sim \mathcal{N}(\mathbf{0}, \mathbf{I})$ 
2 for  $t = T, \dots, 1$  do
3    $\mathbf{z}_t \sim \mathcal{N}(\mathbf{0}, \mathbf{I})$ 
4    $\mathbf{s}'_t \leftarrow \hat{\mathbf{s}}_t + \mathbf{z}_t * \frac{t}{T}$  // diffuse
5    $\hat{\mathbf{s}}_{t-1} \leftarrow \mathbf{s}'_t - \epsilon_\theta(\mathbf{s}'_t, \mathbf{x}, t)$  // denoise
6    $l \leftarrow \|\epsilon_\theta(\mathbf{s}'_t, \mathbf{x}, t) - (\mathbf{s}'_t - \bar{\mathbf{s}})\|^2$ 
7   Update  $\epsilon_\theta$  w.r.t.  $l$ 
8 end

```

Algorithm 2: Training with hierarchical scales

Input: $\mathbf{x} \in \mathbb{R}^{W \times H \times 3}$, RGB image
Input: $\bar{\mathbf{s}} \in \mathbb{R}^{W \times H \times \text{classes}}$, segmentation labels
Parameters: $T \in \mathbb{Z}^1$, number of time steps
Parameters: $M \in \mathbb{Z}^1$, number of scales

```

1  $\hat{\mathbf{s}}_T \sim \mathcal{N}(\mathbf{0}, \mathbf{I})$ 
2 for  $t = T, \dots, 1$  do
3   for  $m = M, \dots, 1$  do
4     Resize  $\hat{\mathbf{s}}_t$  to size  $(\frac{W}{2^{m-1}} \times \frac{H}{2^{m-1}} \times \text{classes})$ 
5     Resize  $\mathbf{x}$  to size  $(\frac{W}{2^{m-1}} \times \frac{H}{2^{m-1}} \times 3)$ 
6      $\mathbf{z}_t \sim \mathcal{N}(\mathbf{0}, \mathbf{I})$ 
7      $\mathbf{s}'_t \leftarrow \hat{\mathbf{s}}_t + \mathbf{z}_t * \frac{t}{T}$  // diffuse
8      $\hat{\mathbf{s}}_{t-1} \leftarrow \mathbf{s}'_t - \epsilon_\theta(\mathbf{s}'_t, \mathbf{x}, t)$  // denoise
9      $l \leftarrow \|\epsilon_\theta(\mathbf{s}'_t, \mathbf{x}, t) - (\mathbf{s}'_t - \bar{\mathbf{s}})\|^2$ 
10    Update  $\epsilon_\theta$  w.r.t.  $l$ 
11  end
12 end

```

3.3. Hierarchical multi-scale diffusion

Performing segmentation at multiple image scales can improve the prediction. We can exploit the propagation artifact from *recursive denoising* using a hierarchical multi-scale denoising process, shown in Algorithm 2.

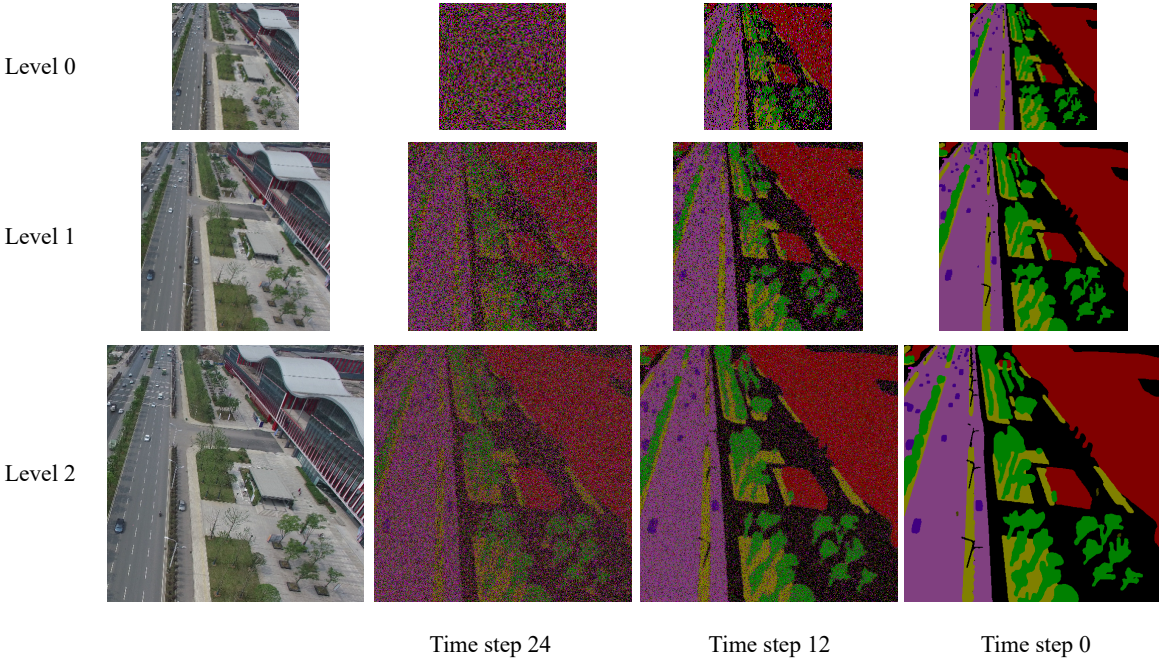


Figure 3. Periodic samples showing the hierarchical multi-scale process. The model progresses through each level (different scale) from level 0, to 2 for every time step. Note the denoising process progresses in reverse time steps, as time steps indicate the noise level. Large structures appear first while finer detail appear later.

At each time step, we run multiple denoising predictions with rescaled inputs. This is done hierarchically, starting from down-scaled inputs we progressively up-scale the inputs and denoise. The scaling schedule contains additional parameters (scaling factor and number of different scaling factors) which can be tuned to specific problems. Fusing the predictions from different image scales, in this manner, lends itself naturally to the denoising process.

The progression of the hierarchical multi-scale denoising process can be seen in Figure 3. It can be seen that large structures appear quickly, even with sharp boundaries. Smaller structures and finer details appear later.

Our approach is also not limited to the scaling schedule used for training, as different scaling schedules can be used during inference. However, we do not explore this option in this paper.

3.4. Architecture

Our model is configured as shown in Figure 2, and consists of four modules; E , F , G and H . Modules F and G encode the input image and the noisy one-hot encoded segmentation, respectively. They share a similar structure, consisting of two ResNetBlocks (as shown in Figure 4) but without any time step embeddings. The output is added together, similar to [1], then fed to H . Module E simply converts the time step to a sinusoidal positional embedding, similar to the positional embeddings of [38]. We take in-

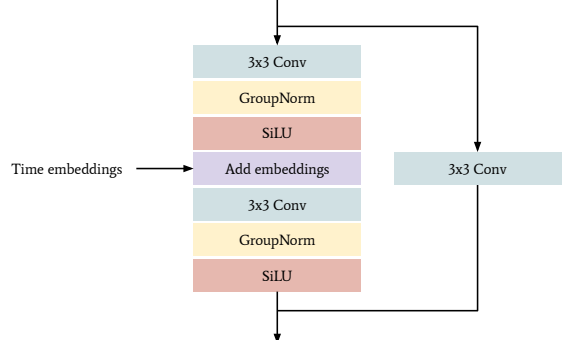


Figure 4. Diagram of our ResNetBlock, consisting of a residual connection [18], a core building block for the model.

spiration from Efficient U-Net [31] to design our encoder-decoder H module, shown in Figure 5. H , combines the time step embeddings at multiple stages through the network (in each ResNetBlock). It also utilizes Efficient Attention [32] which is a type of attention with linear complexity. The output of H is the predicted error (or noise) of the noisy segmentation.

4. Experiments

We focus on semantic segmentation from aerial views and show the benefits of our method. We compare our

Method	Pre-trained	Building	Tree	Clutter	Road	Low Vegetation	Static Car	Moving Car	Human	mIoU
U-Net [30]	No	70.7	67.2	36.1	61.9	32.8	11.2	47.5	0.0	40.9
MS-Dilation [23]	No	74.3	68.1	40.3	63.5	35.5	11.9	42.6	0.0	42.0
FCN-8s [20]	Cityscapes	78.6	73.3	45.3	64.7	46.0	19.7	49.8	0.1	47.2
Dilation Net [41]	Cityscapes	80.7	74.0	45.4	65.1	45.5	24.5	53.6	0.0	48.6
U-Net [30]	Cityscapes	79.0	73.8	46.4	65.3	43.5	26.8	56.6	0.0	48.9
MS-Dilation [23]	Cityscapes	80.9	75.5	46.3	66.7	47.9	22.3	56.9	4.2	50.1
Ours	No	85.1	67.3	54.8	73.3	61.2	54.2	70.5	21.4	61.0

Table 1. Comparison of different methods on UAVid [23]. Results as reported in [23]. Our method achieves the best results across all classes except one and improves on the mIoU.

Method	mIoU	F1-score
DSAC [24]	84.00	-
TDAC [17]	89.16	-
DARNet [9]	88.24	-
SegDiff [1]	91.12	95.14
Ours	92.50	98.68

Table 2. Comparison of different methods on Vaihingen buildings. Results as reported in respective publication. F1-score not reported for some methods.

Description	# of scales	mIoU	F1-score
Recursive + Scales	4	58.98	81.38
Recursive + Scales	3	60.82	82.42
Recursive + Scales	2	60.15	81.52
Recursive	1	57.07	80.70

Table 3. The effects of our proposed hierarchical multi-scale approach on UAVid. The method is relatively sensitive to the number of scales, and three scales provide the best result.

# of time steps	mIoU	F1-score
25	58.98	81.38
15	57.23	81.85
5	56.04	81.78

Table 4. The effects of the number of time steps used during training, on UAVid. Trained with a hierarchy of four scales. More time steps correspond to higher mIoU.

method to U-Net [30], FCN-8s [20], Dilation Net [41] and MS-Dilation [23] on UAVid. For Vaihingen we compare our method to DSAC [24], TDAC [17], DARNet [9] and SegDiff [1].

Data We use UAVid [23], a specialized drone dataset, containing a total of 420 (4K resolution) images from aerial

# of ensembles	mIoU	F1-score
20	60.99	82.48
10	60.93	82.43
5	60.92	82.43
3	60.97	82.47
1	60.82	82.42

Table 5. The effects of using ensembles. The model is not very sensitive to the number of ensembles. Meaning that a single model, which is the most computationally efficient, produces near optimal results.

# of time steps	mIoU	F1-score
25	60.82	82.42
20	60.84	82.44
15	60.83	82.37
10	60.85	82.41
5	60.58	82.21
3	60.05	81.90
1	59.20	81.50

Table 6. The effects of different time steps during inference using a model trained on 25 time steps. This approach allows for efficiency improvements while maintaining high performance.

views. The data is split into sets of 200, 70, and 150 images for training, validation and testing, respectively. There are eight classes; *Building*, *Tree*, *Clutter*, *Road*, *Low Vegetation*, *Static Car*, *Moving Car* and *Human*. For training, we augment the data with random (50%) horizontal flips and randomly (50%) adjust the contrast, saturation and hue by factors of 0.5, 0.5 and 0.05, respectively. In addition, we resize the images to 1024×512 using bilinear interpolation for the image and nearest neighbor interpolation for the segmentation ground truth.

We also experiment on Vaihingen Buildings [11], specifically the setup used in [24], which contains 168 images.

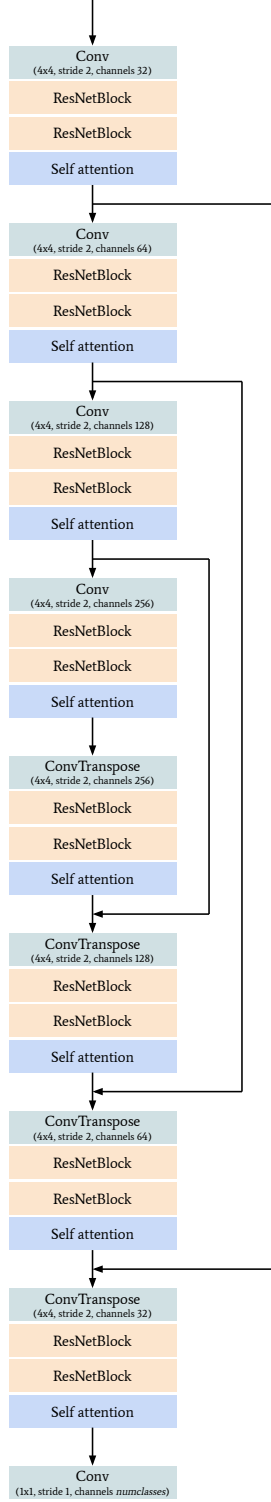


Figure 5. Schematic of our encoder-decoder. The self attention block uses Efficient Attention [32]. The details of the ResNet-Blocks are shown in Figure 4.

These are split between a training set of 100 images and a test set of 68 images. The objective is to label each pixel as either the central building or as background. Multiple buildings can be present in a single image, however, only the building in the center of the image should be labeled. We use the same augmentation strategy as for UAVid but in addition, we also add random (50%) vertical flips.

Metrics We report the Intersection over Union (IoU), also known as the Jaccard Index, for individual classes as well as the mean Intersection over Union (mIoU), averaged over all classes. These metrics are often expressed as percentages.

$$IoU = \frac{TP}{TP + FP + FN} \quad (12)$$

$$mIoU = \frac{1}{N} \sum_{i=1}^N \frac{TP_i}{TP_i + FP_i + FN_i} \quad (13)$$

Where TP , FP and FN are the true positive, false positive and false negative between the predicted and ground truth class labels, respectively. N is the total number of classes in the dataset. We also report the F1-score for the Vaihingen Buildings dataset.

Training Diffusion models tend to use a large number of time steps, in the range of hundreds or thousands [26]. However, we find we can train with far fewer time steps (as low as 5), which directly translates to reduced inference time. However, performance is better when trained with more time steps as can be seen in Table 4, and we train with 25 time steps.

We use AdamW [21] as our optimizer with an initial learning rate of 5×10^{-5} , decay gamma of 0.95 and weight decay of 1×10^{-3} . We use gradient clipping at 1.0 and train for 70 epochs.

Hierarchical multi-scale We explore the effectiveness of our hierarchical multi-scale approach in Table 3. Each scale level reduces the image size by half. We find our hierarchical multi-scale approach to provide a large improvement over the baseline. We find that using three scale levels results in optimal performance, but using too many negates most of the benefits.

Ensemble Generative diffusion models are dependent on the input noise. We experiment with combining multiple runs (with different random noise), and averaging the results (Table 5). This approach provides only marginally better results, meaning our method is not negatively dependent on the input noise. Using an ensemble requires more computational resources, compared to only a single run, and therefore not an efficient use of computational budget.

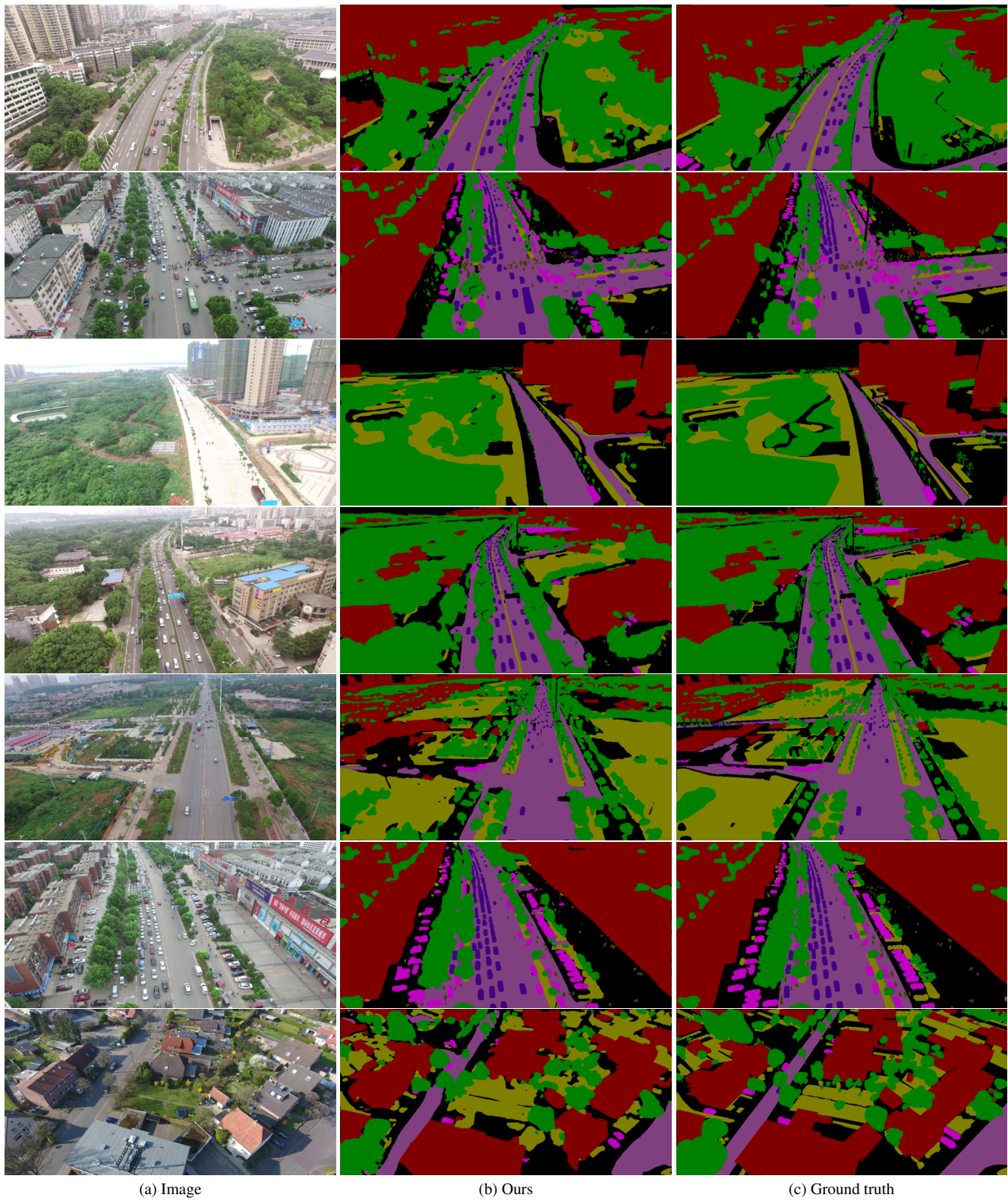


Figure 6. Qualitative results on UAVid [23]. Our method can detect small details such as street lights, tree branches and people.

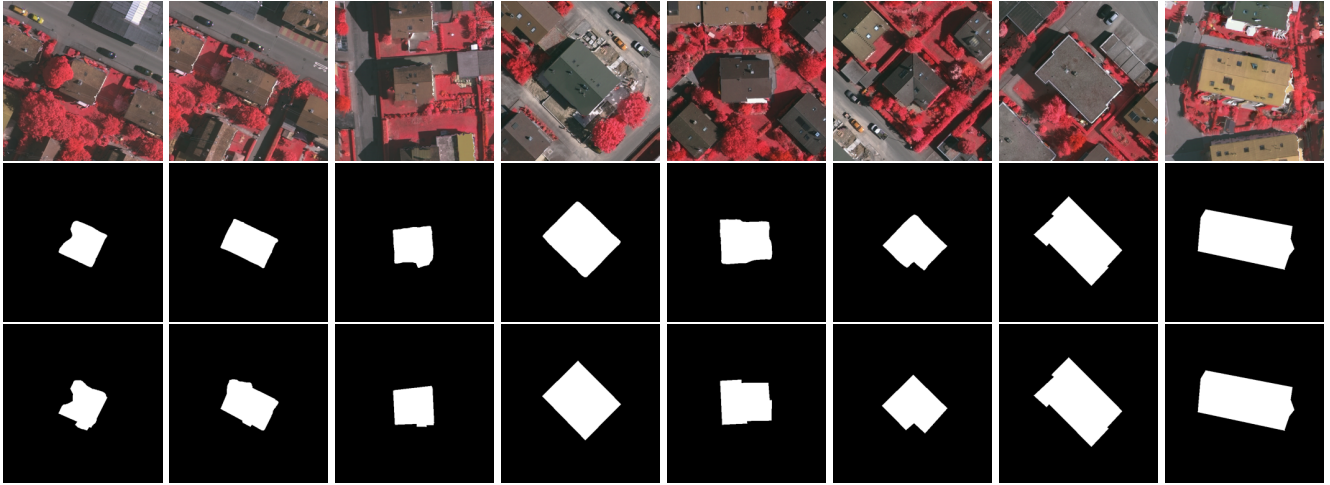


Figure 7. Qualitative results on Vaihingen Buildings [11]. First row: input image, middle row: our method, bottom row: ground truth.

Comparison to other methods We compare our method to other methods on both UAVid and Vaihingen. For UAVid, we produce the best results for all classes except one, and we beat the previous best average result (mIoU) by a large margin (Table 1). Qualitative results are shown in Figure 6. Our method can detect small details such as people in the distance, street lights and tree branches. Qualitative results on Vaihingen are shown in Figure 7. Our method produces results with sharp edges but occasionally with slightly rounded corners. Table 2 shows qualitative results on Vaihingen, where we achieve the best mIoU.

Skip time steps We also explore skipping time steps during inference, to increase the efficiency of our method, shown in Table 6. This is possible using Equation (10). We notice, we can reduce the number of time steps by 50% with no effect on performance. Beyond that, only a slight decrease in performance is observed. This means our method can be trained with a high number of time steps and be made more efficient during inference, without loss of performance.

5. Discussion

Our method performs especially well on UAVid compared to models not pre-trained on Cityscapes [10], indicating our method generalizes much better. We believe this is the result of *recursive denoising*, as learning on repeated training data samples (once per epoch) results in regularization. In other words, the recursive denoising process augments the observed training sample. We did not experience any issues with over-fitting when using *recursive denoising*, however, the training and validation results did plateau. This could mean our hyperparameter selection is not optimal and additional performance could be achieved.

Our results are very positive as they indicate that diffusion models can remove most of the Gaussian noise correctly, and prevent the need of using multiple runs (ensemble), which is inefficient. In addition, the fact that reducing the number of time steps during inference by 50% without any loss to performance makes our diffusion model relatively efficient. Further, using only a single inference run still produces competitive results, which means our method can be used in practice.

Diffusion models for segmentation are a new class of segmentation models, which we believe will open a new chapter on this task.

6. Conclusion

In this work, we present *recursive denoising* along with a hierarchical multi-scale diffusion model for semantic segmentation from aerial views. *Recursive denoising* allows for information to propagate during the denoising process. We observe that our diffusion model is resilient to variations to input noise and can be relatively efficient by skipping time steps during inference without losing performance. We show our proposed solution yields state-of-the-art results on UAVid and Vaihingen Buildings. We believe our *recursive denoising* diffusion model is only the first step of a new promising class of segmentation models.

References

[1] Tomer Amit, Eliya Nachmani, Tal Shaharbany, and Lior Wolf. Segdiff: Image segmentation with diffusion probabilistic models. *arXiv preprint arXiv:2112.00390*, 2021. 2, 4, 5

[2] Arpit Bansal, Eitan Borgnia, Hong-Min Chu, Jie S Li, Hamid Kazemi, Furong Huang, Micah Goldblum, Jonas Geiping, and Tom Goldstein. Cold diffusion: Inverting arbitrary image transforms without noise. *arXiv preprint arXiv:2208.09392*, 2022. 2

[3] Dmitry Baranckuk, Ivan Rubachev, Andrey Voynov, Valentin Khrulkov, and Artem Babenko. Label-efficient semantic segmentation with diffusion models. *arXiv preprint arXiv:2112.03126*, 2021. 2

[4] Bilel Benjdira, Yakoub Bazi, Anis Koubaa, and Kais Ouni. Unsupervised domain adaptation using generative adversarial networks for semantic segmentation of aerial images. *Remote Sensing*, 11(11):1369, 2019. 2

[5] Liang-Chieh Chen, George Papandreou, Iasonas Kokkinos, Kevin Murphy, and Alan L Yuille. Semantic image segmentation with deep convolutional nets and fully connected crfs. *arXiv preprint arXiv:1412.7062*, 2014. 2

[6] Liang-Chieh Chen, George Papandreou, Iasonas Kokkinos, Kevin Murphy, and Alan L Yuille. Deeplab: Semantic image segmentation with deep convolutional nets, atrous convolution, and fully connected crfs. *IEEE transactions on pattern analysis and machine intelligence*, 40(4):834–848, 2017. 2

[7] Liang-Chieh Chen, Yi Yang, Jiang Wang, Wei Xu, and Alan L Yuille. Attention to scale: Scale-aware semantic image segmentation. In *Proceedings of the IEEE conference on computer vision and pattern recognition*, pages 3640–3649, 2016. 1, 2

[8] Liang-Chieh Chen, Yukun Zhu, George Papandreou, Florian Schroff, and Hartwig Adam. Encoder-decoder with atrous separable convolution for semantic image segmentation. In *Proceedings of the European conference on computer vision (ECCV)*, pages 801–818, 2018. 2

[9] Dominic Cheng, Renjie Liao, Sanja Fidler, and Raquel Urtasun. Darnet: Deep active ray network for building segmentation. In *Proceedings of the IEEE/CVF Conference on Computer Vision and Pattern Recognition*, pages 7431–7439, 2019. 5

[10] Marius Cordts, Mohamed Omran, Sebastian Ramos, Timo Rehfeld, Markus Enzweiler, Rodrigo Benenson, Uwe Franke, Stefan Roth, and Bernt Schiele. The cityscapes dataset for semantic urban scene understanding. In *Proceedings of the IEEE conference on computer vision and pattern recognition*, pages 3213–3223, 2016. 8

[11] Michael Cramer. The dgpf-test on digital airborne camera evaluation overview and test design. *Photogrammetrie-Fernerkundung-Geoinformation*, pages 73–82, 2010. 1, 5, 8

[12] Florinel-Alin Croitoru, Vlad Hondu, Radu Tudor Ionescu, and Mubarak Shah. Diffusion models in vision: A survey. *arXiv preprint arXiv:2209.04747*, 2022. 2

[13] Prafulla Dhariwal and Alexander Nichol. Diffusion models beat gans on image synthesis. *Advances in Neural Information Processing Systems*, 34:8780–8794, 2021. 2

[14] Clement Farabet, Camille Couprie, Laurent Najman, and Yann LeCun. Learning hierarchical features for scene labeling. *IEEE transactions on pattern analysis and machine intelligence*, 35(8):1915–1929, 2012. 1

[15] Dario Floreano and Robert J Wood. Science, technology and the future of small autonomous drones. *nature*, 521(7553):460–466, 2015. 1

[16] Ian Goodfellow, Jean Pouget-Abadie, Mehdi Mirza, Bing Xu, David Warde-Farley, Sherjil Ozair, Aaron Courville, and Yoshua Bengio. Generative adversarial nets. In *Advances in Neural Information Processing Systems*, volume 27, 2014. 2

[17] Ali Hatamizadeh, Debleena Sengupta, and Demetri Terzopoulos. End-to-end trainable deep active contour models for automated image segmentation: Delineating buildings in aerial imagery. In *European Conference on Computer Vision*, pages 730–746. Springer, 2020. 5

[18] Kaiming He, Xiangyu Zhang, Shaoqing Ren, and Jian Sun. Deep residual learning for image recognition. In *Proceedings of the IEEE conference on computer vision and pattern recognition*, pages 770–778, 2016. 4

[19] Jonathan Ho, Ajay Jain, and Pieter Abbeel. Denoising diffusion probabilistic models. *Advances in Neural Information Processing Systems*, 33:6840–6851, 2020. 2, 3

[20] Jonathan Long, Evan Shelhamer, and Trevor Darrell. Fully convolutional networks for semantic segmentation. In *Proceedings of the IEEE conference on computer vision and pattern recognition*, pages 3431–3440, 2015. 2, 5

[21] Ilya Loshchilov and Frank Hutter. Decoupled weight decay regularization. *arXiv preprint arXiv:1711.05101*, 2017. 6

[22] Pauline Luc, Camille Couprie, Soumith Chintala, and Jakob Verbeek. Semantic segmentation using adversarial networks. *arXiv preprint arXiv:1611.08408*, 2016. 2

[23] Ye Lyu, George Vosselman, Gui-Song Xia, Alper Yilmaz, and Michael Ying Yang. Uavid: A semantic segmentation dataset for uav imagery. *ISPRS Journal of Photogrammetry and Remote Sensing*, 165:108–119, 2020. 1, 5, 7

[24] Diego Marcos, Devis Tuia, Benjamin Kellenberger, Lisa Zhang, Min Bai, Renjie Liao, and Raquel Urtasun. Learning deep structured active contours end-to-end. In *Proceedings of the IEEE Conference on Computer Vision and Pattern Recognition*, pages 8877–8885, 2018. 5

[25] Mohammadreza Mostajabi, Payman Yadollahpour, and Gregory Shakhnarovich. Feedforward semantic segmentation with zoom-out features. In *Proceedings of the IEEE conference on computer vision and pattern recognition*, pages 3376–3385, 2015. 1

[26] Alexander Quinn Nichol and Prafulla Dhariwal. Improved denoising diffusion probabilistic models. In *International Conference on Machine Learning*, pages 8162–8171. PMLR, 2021. 2, 3, 6

[27] Chao Peng, Xiangyu Zhang, Gang Yu, Guiming Luo, and Jian Sun. Large kernel matters—improve semantic segmentation by global convolutional network. In *Proceedings of the IEEE conference on computer vision and pattern recognition*, pages 4353–4361, 2017. 2

[28] Aditya Ramesh, Prafulla Dhariwal, Alex Nichol, Casey Chu, and Mark Chen. Hierarchical text-conditional image generation with clip latents. *arXiv preprint arXiv:2204.06125*, 2022. [2](#)

[29] Robin Rombach, Andreas Blattmann, Dominik Lorenz, Patrick Esser, and Björn Ommer. High-resolution image synthesis with latent diffusion models. In *Proceedings of the IEEE/CVF Conference on Computer Vision and Pattern Recognition*, pages 10684–10695, 2022. [2](#)

[30] Olaf Ronneberger, Philipp Fischer, and Thomas Brox. U-net: Convolutional networks for biomedical image segmentation. In *International Conference on Medical image computing and computer-assisted intervention*, pages 234–241. Springer, 2015. [1, 5](#)

[31] Chitwan Saharia, William Chan, Saurabh Saxena, Lala Li, Jay Whang, Emily Denton, Seyed Kamyar Seyed Ghasemipour, Burcu Karagol Ayan, S Sara Mahdavi, Rapha Gontijo Lopes, et al. Photorealistic text-to-image diffusion models with deep language understanding. *arXiv preprint arXiv:2205.11487*, 2022. [2, 4](#)

[32] Zhuoran Shen, Mingyuan Zhang, Haiyu Zhao, Shuai Yi, and Hongsheng Li. Efficient attention: Attention with linear complexities. In *Proceedings of the IEEE/CVF winter conference on applications of computer vision*, pages 3531–3539, 2021. [4, 6](#)

[33] Jascha Sohl-Dickstein, Eric Weiss, Niru Maheswaranathan, and Surya Ganguli. Deep unsupervised learning using nonequilibrium thermodynamics. In *International Conference on Machine Learning*, pages 2256–2265. PMLR, 2015. [2](#)

[34] Nasim Souly, Concetto Spampinato, and Mubarak Shah. Semi supervised semantic segmentation using generative adversarial network. In *Proceedings of the IEEE international conference on computer vision*, pages 5688–5696, 2017. [2](#)

[35] Robin Strudel, Ricardo Garcia, Ivan Laptev, and Cordelia Schmid. Segmenter: Transformer for semantic segmentation. In *Proceedings of the IEEE/CVF International Conference on Computer Vision (ICCV)*, pages 7262–7272, October 2021. [2](#)

[36] Andrew Tao, Karan Sapra, and Bryan Catanzaro. Hierarchical multi-scale attention for semantic segmentation. *arXiv preprint arXiv:2005.10821*, 2020. [1, 2](#)

[37] Marco Toldo, Andrea Maracani, Umberto Michieli, and Pietro Zanuttigh. Unsupervised domain adaptation in semantic segmentation: a review. *Technologies*, 8(2):35, 2020. [2](#)

[38] Ashish Vaswani, Noam Shazeer, Niki Parmar, Jakob Uszkoreit, Llion Jones, Aidan N Gomez, Łukasz Kaiser, and Illia Polosukhin. Attention is all you need. *Advances in neural information processing systems*, 30, 2017. [2, 4](#)

[39] Enze Xie, Wenjia Wang, Wenhui Wang, Peize Sun, Hang Xu, Ding Liang, and Ping Luo. Segmenting transparent object in the wild with transformer. *arXiv preprint arXiv:2101.08461*, 2021. [2](#)

[40] Enze Xie, Wenhui Wang, Zhiding Yu, Anima Anandkumar, Jose M Alvarez, and Ping Luo. Segformer: Simple and efficient design for semantic segmentation with transformers. *Advances in Neural Information Processing Systems*, 34:12077–12090, 2021. [2](#)

[41] Fisher Yu and Vladlen Koltun. Multi-scale context aggregation by dilated convolutions. *arXiv preprint arXiv:1511.07122*, 2015. [5](#)

[42] Xinming Zhang, Xiaobin Zhu, Naiguang Zhang, Peng Li, Lei Wang, et al. Seggan: Semantic segmentation with generative adversarial network. In *2018 IEEE Fourth International Conference on Multimedia Big Data (BigMM)*, pages 1–5. IEEE, 2018. [2](#)

[43] Hengshuang Zhao, Jianping Shi, Xiaojuan Qi, Xiaogang Wang, and Jiaya Jia. Pyramid scene parsing network. In *Proceedings of the IEEE conference on computer vision and pattern recognition*, pages 2881–2890, 2017. [2](#)

[44] Sixiao Zheng, Jiachen Lu, Hengshuang Zhao, Xiatian Zhu, Zekun Luo, Yabiao Wang, Yanwei Fu, Jianfeng Feng, Tao Xiang, Philip HS Torr, et al. Rethinking semantic segmentation from a sequence-to-sequence perspective with transformers. In *Proceedings of the IEEE/CVF conference on computer vision and pattern recognition*, pages 6881–6890, 2021. [2](#)